Sci

MDPI

Article

Exploring Anti-Inflammatory and Anti-Tyrosinase Potentials and Phytochemical Profiling of *Cannabis sativa* Stems Byproducts

Pannita Kongtananeti [1], Desy Liana [1], Hla Myo [1], Anuchit Phanumartwiwath [1,*] and Chitlada Areesantichai [1,2,*]

[1] College of Public Health Sciences, Chulalongkorn University, Bangkok 10330, Thailand; ppunch.k@gmail.com (P.K.); desyliana13@gmail.com (D.L.); hlamyo.dr1996@gmail.com (H.M.)
[2] Excellent Center for Health and Social Sciences and Addiction Research, Chulalongkorn University, Bangkok 10330, Thailand
* Correspondence: anuchit.p@chula.ac.th (A.P.); chitlada.a@chula.ac.th (C.A.); Tel.: +66-2-218-8194 (C.A.)

Abstract: *Cannabis sativa* L. has been traditionally used for its therapeutic properties, particularly in treating various skin conditions. This study explores the in vitro anti-aging potential of five distinct parts of *C. sativa* L. (inflorescence, seed, leaf, stem, and root) by analyzing their bioactive compounds and biological activities. Ultrasound-assisted extraction was employed using ethyl acetate as an extracting solvent, followed by chemical characterization via gas chromatography-mass spectrometry (GC-MS/MS) and liquid chromatography quadrupole time-of-flight mass spectrometry (LC-QTOF-MS/MS) analyses. The biological assessment included antioxidant, anti-inflammatory, anti-tyrosinase activities, and cytotoxicity evaluations. The inflorescence extract demonstrated the antioxidant activity, with a half-maximal inhibitory concentration (IC_{50}) value of 3,849.01 ± 5.25 µg/mL against DPPH radicals and 31.19 ± 0.96% inhibition of NO radicals at 1.25 mg/mL. Notably, the stem extract exhibited the highest anti-tyrosinase activity, with an IC_{50} value of 0.01 ± 0.00 mg/mL, and significantly inhibited 5-lipoxygenase (5-LOX) activity with an IC_{50} value of <0.024 µg/mL. All extracts showed no cytotoxicity on HaCaT cells at a concentration of 10 µg/mL, indicating their potential safety for dermatological applications. The stem extract was abundant in phytosterols, triterpenoids, diterpenoids, unsaturated fatty acids, and phenolic compounds, which likely contribute to its anti-inflammatory and anti-tyrosinase effects. These findings suggest that the stem, traditionally considered as waste, could be a valuable raw material for developing dermatological treatments with strong anti-inflammatory and skin-brightening effects.

Keywords: antioxidant; anti-inflammatory; anti-tyrosinase; *Cannabis sativa*; mass spectroscopy; ultrasound-assisted extraction

Received: 22 March 2025
Revised: 7 May 2025
Accepted: 23 May 2025
Published: 3 June 2025

Citation: Kongtananeti, P.; Liana, D.; Myo, H.; Phanumartwiwath, A.; Areesantichai, C. Exploring Anti-Inflammatory and Anti-Tyrosinase Potentials and Phytochemical Profiling of *Cannabis sativa* Stems Byproducts. *Sci* **2025**, *7*, 77. https://doi.org/10.3390/sci7020077

1. Introduction

In recent years, the increasing recognition of the effects of skin aging on aesthetic appearance and dermal health has contributed to a marked rise in the demand for anti-aging products. As people age, they experience a range of skin changes, including wrinkles, hyperpigmentation, and reduced elasticity. These changes are caused by intrinsic factors such as hormonal imbalances and cellular metabolism, as well as extrinsic factors like ultraviolet radiation, pollution, and environmental toxins.

Accumulation of oxidative damage in cells is a major contributor to skin aging [1,2]. Beyond the physical effects, skin aging can also have profound psychological and social consequences, often leading to reduced self-esteem and diminished quality of life. Skin

conditions such as melasma and acne, which often worsen with age, further highlight the importance of treatments that address both aesthetic and health concerns [3]. As a result, the demand for innovative anti-aging products is growing, with consumers looking for solutions to both minimize visible signs of aging and improve overall skin health, promoting a youthful appearance and well-being.

In response to the growing demand for natural skincare products, *Cannabis sativa* L., a plant long used in traditional medicine, has emerged as a promising option for modern dermatological treatments. As a member of the Cannabaceae family, *C. sativa* is well-known for its various applications, particularly in the pharmaceutical industry, where it has been used to treat skin infections and other health conditions [4].

Tyrosinase is considered a key enzyme in melanin biosynthesis, catalyzing the oxidation of L-tyrosine to L-dopaquinone, a precursor in melanin synthesis, which plays a role in skin aging development [5,6]. Tyrosinase activity leads to age spots and hyperpigmentation, which are common characteristics of aged skin. Tyrosinase inhibitors are known to regulate melanin synthesis, reducing the occurrence of hyperpigmentation and promoting brighter skin [7]. The demand for tyrosinase-inhibiting agents is increasing in cosmeceutical products aimed at maintaining skin health and brightness. In addition, reactive oxygen species (ROS) can activate tyrosinase and increase DNA damage, leading to enhanced melanogenesis and melanocyte proliferation. Furthermore, pro-inflammatory mediators can accelerate the aging process. Accordingly, the use of anti-tyrosinase, antioxidant, and anti-inflammatory agents in skincare products is beneficial for reducing hyperpigmentation and slowing the skin aging process [8–10].

The plant's medicinal potential is largely due to its rich variety of secondary metabolites, including cannabinoids such as cannabidiol (CBD), as well as terpenes and flavonoids. These compounds have demonstrated strong anti-inflammatory, antipruritic, and antioxidant effects, making *C. sativa* L. a valuable resource for developing treatments for skin conditions like hyperpigmentation by inhibiting tyrosinase, a key enzyme in melanin production [4].

To effectively harness the therapeutic potential of *C. sativa* L., it is important to employ a suitable extraction method capable of preserving the integrity of its bioactive compounds. Given the complexity of *C. sativa* L. bioactive compounds, ultrasound-assisted extraction (UAE) has been chosen for this study due to its advantages over traditional extraction methods. UAE works by using ultrasonic waves to break down plant cell walls, enhancing the dissolution and diffusion of solutes. This process improves both the yield and quality of the extracted compounds [11]. Thus, UAE has been employed for isolating the delicate secondary metabolites from *C. sativa* L.

Examining biological activity and bioactive compound profiles of various parts of *C. sativa* L., such as seeds, leaves, inflorescences, stems, and roots, can significantly contribute to exploring its therapeutic potential. Research suggests that these different parts may contain varying levels of cannabinoids, terpenoids, and flavonoids, each contributing uniquely to the plant's medicinal properties [4]. Despite the well-documented benefits of *C. sativa* L. [12–15], comprehensive studies that explore the anti-aging potential of these different plant parts, particularly in relation to tyrosinase inhibition and other skin-related benefits, are still limited.

Skin aging is a multifactorial biological process that is influenced by various factors, including inflammation, oxidative stress, and dysfunction of skin structural components [10,16]. Therefore, this study aims to assess the in vitro antioxidant, anti-inflammatory, skin-related enzyme inhibitory, and cytotoxic properties of extracts derived from seeds, leaves, inflorescences, stems, and roots of *C. sativa* L., further, we investigate the major bioactive compounds in *C. sativa* L. using mass spectrometry techniques such as

gas and liquid chromatography with mass spectrometry. By systematically exploring these plant parts, the research intends to pinpoint the most promising candidate from *C. sativa*, including their by-products (e.g., roots and stems), for developing natural and effective skincare products, particularly for skin aging and brightener products.

2. Materials and Methods

2.1. Chemicals

All reagents used in this study were sourced from reputable suppliers. Quercetin hydrate, gallic acid, sodium nitroprusside (SNP) dihydrate, sulfanilamide, *N*-(1-naphthyl) ethylenediamine dihydrochloride, tyrosinase from mushroom, and L-Dopa ethyl ester were purchased from Sigma Chemical Co. (St. Louis, MO, USA). Human recombinant 5-LOX enzyme was obtained from Cayman Chemical (Ann Arbor, MI, USA), and nordihydroguaiaretic acid (NDGA) was procured from Tokyo Chemical Industry (Tokyo, Japan). Ethyl acetate and methanol, used as solvents, were obtained from RCI Labscan (Bangkok, Thailand), while acetonitrile was sourced from Honeywell's Burdick & Jackson (B&J) (Chemex, Thailand).

2.2. Plant Materials and Sample Preparation

Five parts of *C. sativa* L., including seeds, leaves, inflorescences, stems, and roots, were obtained from the Drug Dependence Research Center, College of Public Health Sciences, at the Centre of Learning Network for the Region (CLNR), Chulalongkorn University, Saraburi, Thailand. The plant parts were dried in a tray dryer at 45 °C for three days, then ground into a fine powder using a mechanical grinder. The powdered material was stored at room temperature for further analysis.

2.3. Ultrasonic-Assisted Extraction of Cannabis sativa L.

Each part of *C. sativa* L. was subjected to extraction using ethyl acetate in an ultrasonic bath (Shanghai Kudos Ultrasonic Instrument Co., Ltd., Shanghai, China). The UAE method followed the procedure outlined by Jan Rožanc et al. [17]. The extraction was conducted with a material-to-solvent ratio of 1:10 (10 g of plant material in 100 mL of solvent) at a controlled temperature of 40 °C (±1 °C). Ultrasonic irradiation was performed for 120 min at 53 kHz and 100 W with a 50% duty cycle, consisting of alternating 5 min of sonication and 5 min of rest. The ethyl acetate extracts were concentrated under reduced pressure to obtain individual extracts while minimizing potential errors in bioactivity assays caused by residual ethyl acetate in the samples. The yield of each extract was evaluated as follows:

$$\% \text{ Yield} = \frac{\text{weight of extract (g)}}{\text{weight of dried plant material used (g)}} \times 100 \quad (1)$$

2.4. Determination of Total Phenolic Content (TPC) and Total Flavonoids Content (TFC)

The TPC and TFC of all *C. sativa* L. extracts were determined using the method described in our previous study [18]. For TPC analysis, all extracts were diluted with water to a final concentration of 0.25 mg/mL. After adding each extract to the wells, 10% Folin-Ciocâlteu reagent was applied. A solution of 7.5% sodium carbonate was added after a 20-min incubation in the dark at room temperature, followed by another 20-min incubation. The absorbance was then measured at 756 nm. The assay was carried out in triplicates. The calibration curve of gallic acid was determined (Figure S1). The TPC values were presented as mg gallic acid equivalent per gram of dry extract (mg GAE/g dry extract). For TFC analysis, all extracts were diluted with water to a final concentration of 0.25 mg/mL. After adding each extract to the wells, 10% aluminum chloride solution, ethanol, and 1M sodium acetate solution were added. The mixture was incubated for

40 min at room temperature in the dark. The absorbance was measured at 415 nm. The assay was carried out in triplicates. The calibration curve of quercetin was determined (Figure S2). The TFC values were presented as mg quercetin equivalent per gram of dry extract (mg QE/g dry weight).

2.5. 2,2-Diphenyl-1-Picrylhydrazyl (DPPH) and Nitric Oxide (NO) Radical Scavenging Activities

The DPPH and NO radical scavenging capacity of the *C. sativa* L. extracts was evaluated according to the method stated by our previous study [18]. For DPPH analysis, all samples were diluted in DMSO at various concentrations ranging from 5 mg/mL to 0.15625 mg/mL. Each extract (20 µL) was added to each well of a 96-well plate, followed by the addition of 180 µL of 120 µM DPPH solution in methanol. The plate was incubated for 30 min at 37 °C in the dark. The absorbance was measured at 517 nm using a microplate reader. The NO radical-scavenging activity was determined using the Griess reaction. Samples were diluted in DMSO (0.156–5 mg/mL) and reacted with 10 mM sodium nitroprusside (SNP) in PBS (pH 7.3) for 90 min under visible light at room temperature. After incubation, 50 µL of 1% sulfanilamide in 5% H_3PO_4 was added, followed by 50 µL of 0.1% *N*-(1-naphthyl)-ethylenediamine (NED) solution. The mixture was incubated in the dark for 30 min, producing a magenta chromophore through a diazotization-coupling reaction. Absorbance was measured at 540 nm using a microplate reader. The assay was carried out in triplicates. Quercetin was used as a positive control for DPPH and NO analysis, and the radical scavenging activity was calculated using the formula:

$$\text{Inhibition } (\%) = \frac{\text{Absorbance control} - \text{Absorbance sample}}{\text{Absorbance control}} \times 100 \quad (2)$$

2.6. 5-Lipoxygenase (5-LOX) Inhibition of the C. sativa L. Extracts

The anti-inflammatory properties of *C. sativa* L. extracts were assessed using a 5-LOX inhibition assay, according to the protocol stated in our previous study [18]. Human recombinant 5-lipoxygenase (5-LOX) was utilized in the assay. Various concentrations (20 µL) of the test compounds, dissolved in a mixture of polysorbate-20 and DMSO, were initially added to 100 µL of 0.1 M potassium phosphate buffer (pH 6.3). The resulting mixture was maintained at 25 °C, after which 20 µL of the 5-LOX enzyme solution (100 U in 0.1 M potassium phosphate buffer, pH 6.3) was introduced, followed by a 4-min pre-incubation. The enzymatic reaction was initiated by the addition of 10 µL of 1 mM arachidonic acid, serving as the substrate. After a 30-min incubation period at 25 °C, the absorbance was recorded at 234 nm. All experiments were performed in triplicate. Nordihydroguaiaretic acid (NDGA) was used as the positive control, and percentage inhibition was determined using the Formula (2).

2.7. In Vitro Anti-Tyrosinase Activity of the C. sativa L. Extracts

The anti-tyrosinase activity of the extracts was evaluated using a modified dopachrome method based on the work of Manosroi et al. [19]. The *C. sativa* L. extracts were diluted in 10% DMSO, with kojic acid serving as a positive control. The reaction mixture included 40 µL of the extract, 40 µL of 0.1 mg/mL L-tyrosinase, 50 µL of mushroom tyrosinase, and 80 µL of 0.1 M phosphate buffer (PBS). The mixture was incubated at 37 °C for 60 min, and absorbance was determined at 570 nm. The assay was carried out in triplicates. The percentage inhibition was calculated using the Formula (2).

2.8. Cytotoxicity of the C. sativa L. Extracts on Human Keratinocyte (HaCaT) Cells

The cytotoxicity of different extracts was evaluated by using the MTT assay on HaCaT cells according to the protocol outlined by Wan et al. [20]. HaCaT keratinocyte cells were

cultured in Dulbecco's Modified Eagle Medium (DMEM) supplemented with 10% fetal bovine serum (FBS), 100 U/mL penicillin, and 100 µg/mL streptomycin, and maintained at 37 °C in a humidified incubator with 5% CO_2. Approximately 10,000 cells were seeded into each well of a 96-well plate and incubated for 24 h to allow cell adherence. Subsequently, the cells were treated with varying concentrations (5, 10, and 20 µg/mL) of *Cannabis sativa* L. extracts for another 24-h period. Following treatment, MTT reagent was added to each well, and the plates were incubated for 2 to 3 h. The resulting formazan crystals were solubilized using DMSO, and absorbance was recorded at 570 nm. Experiments were performed in triplicate, and the percentage of cell viability was calculated as outlined in the formula.

$$\text{Cell viability } (\%) = \frac{\text{Absorbance treated cells}}{\text{Absorbance control cells}} \times 100 \quad (3)$$

2.9. Gas Chromatography-Mass Spectrometry (GC-MS/MS) Analysis

All *Cannabis sativa* L. ethyl acetate extracts were analyzed using a triple quadrupole gas chromatography-tandem mass spectrometry (GC-MS/MS) system (Agilent Technologies, Santa Clara, CA, USA), conducted at the Scientific and Technological Research Equipment Center (STREC), Chulalongkorn University. The analysis was performed on an Agilent 7890 GC system coupled with a 7000C QQQ mass spectrometer, equipped with an HP-5ms capillary column (30 m × 0.25 mm i.d., 0.25 µm film thickness, part no. 19091S-433UI). A single quadrupole operated in scan mode was used for qualitative compound identification, with the method adapted and modified from a previous study [21]. Ultra-high-purity helium (99.99%) served as the carrier gas at a constant flow rate of 1 mL/min. The injector temperature was set at 250 °C with a split ratio of 10:1. A 1.0 µL sample volume (10 mg/mL in dichloromethane) was injected. The temperature program initiated at 60 °C (held for 2 min), increased at 3 °C/min to 165 °C, then ramped at 5 °C/min to 300 °C and held for 15 min, resulting in a total run time of 79 min. All analyses were conducted in triplicate. The mass spectrometer operated in electron impact (EI) ionization mode at 70 eV, and data were acquired in scan mode across the 33–500 m/z range, and component identification of the extracts was obtained by comparing both the mass spectra and retention index (RI) against the National Institute of Standards and Technology library (NIST2020) library. The RI of the n-alkane series (C8–C36) was used to compute the RI values. A matching score of more than 60 and an RI value difference of less than 20 units between the calculated RI and the database values for the same stationary phase were required for compound identification. Data acquisition and peak integration were managed using MassHunter WorkStation Qualitative Analysis Version 10.0, 2018.

2.10. Liquid Chromatography Quadrupole Time-of-Flight Mass Spectrometry (LC-QTOF-MS/MS) Analysis

The ethyl acetate extracts were further analyzed using LC-QTOF-MS/MS under the conditions outlined in a previous study [22]. Liquid chromatography was carried out using an ExionLC™ AD ultra-high-performance liquid chromatography (UHPLC) system (SCIEX, Framingham, MA, USA), while mass spectrometric analysis was performed with an X500R QTOF system (SCIEX, Framingham, MA, USA). Chromatographic separation was performed using Kinetex® C18 column (100 × 2.1 mm, 2.6 µm; Phenomenex, Torrance, CA, USA), which was thermostated at 34 °C. The condition was adapted and modified from the previous study. The mobile phase system consisted of water containing 5% acetonitrile (Phase A) and acetonitrile containing 5% water (Phase B), with both phases supplemented with 0.1% formic acid to facilitate ionization. The liquid chromatography pump was set to deliver the mobile phase at a flow rate of 0.5 mL/min. The gradient elution profile was as follows: Phase B was maintained at 4% from 0 to 1 min; increased from 4% to 20% between

1 and 5 min; then gradually raised from 20% to 70% between 5 and 10 min; followed by an increase from 70% to 90% between 10 and 20 min; then from 90% to 100% between 20 and 32 min; and finally held at 100% Phase B from 32 to 42 min. The electrospray ionization (ESI) source was operated in positive ion mode. Both MS and MS/MS data were acquired in positive polarity using centroid mode. High-resolution mass spectra were obtained in MS and MS/MS scans across an m/z range of 50–1100. Data processing and analysis were conducted using SCIEX OS software version 3.3.0.12027 (AB SCIEX^{TM}, Framingham, MA, USA). Compound identification was carried out using the NIST2017 library, with a minimum similarity threshold of 95%.

2.11. Statistical Analysis

All experiments, including assessments of antioxidant activity, enzyme inhibitory assays, cell viability tests, and bioactive compound determinations, were conducted in triplicate. The data are presented as mean values ± standard deviation (SD). Statistical analyses were performed using one-way ANOVA, followed by Duncan's post hoc test, with a significance threshold set at p-value < 0.05. The analyses were conducted using IBM SPSS, Version 28.

3. Results and Discussion

3.1. Extraction of the C. sativa L. Extracts

The percentage yields of *C. sativa* L. extracts obtained from five different plant parts using ethyl acetate through UAE are presented in Table 1. The extract from *C. sativa* L. seeds (CSE) exhibited the highest yield at 20.01%, whereas the extracts from the other parts yielded lower percentages. The seed extract appeared as a brownish dark green viscous liquid, differing from the crude extracts of other plant parts. Specifically, the inflorescence extract was a brownish dark green semi-solid, while the leaf, stem, and root extracts were greenish yellow semi-solids. All extracts were stored in amber vials at −20 °C for further use. The notably higher yield from the seed extract may be due to the rich content of fatty acids and other lipophilic compounds within the seeds, which are efficiently extracted by ethyl acetate. This is consistent with previous studies, which reported a 6.8% yield for *C. sativa* L. seed n-hexane extract in an oil form [23]. The yields from the other plant parts—leaves, inflorescences, stems, and roots—were lower, which may be due to the differing compositions of these tissues. This variability in yield highlights the distinct chemical compositions of the different plant parts, each contributing uniquely to the overall profile of bioactive compounds in *C. sativa* L. Ethyl acetate was chosen for the extraction solvent due to its moderate polarity, which can extract a wide range of bioactive compounds from polar to non-polar molecules such as phenolic compounds, flavonoids, terpenes, and cannabinoids.

Table 1. Percent yields of the *C. sativa* L. extracts.

Extract	Percent Yield (%)
C. sativa L. seed (CSE)	20.01
C. sativa L. inflorescence (CIF)	6.62
C. sativa L. leaf (CLE)	3.46
C. sativa L. stem (CST)	0.28
C. sativa L. root (CRO)	0.23

3.2. Biological Assessment of the C. sativa L. Extracts

3.2.1. Determination of Total Phenolic and Total Flavonoids Contents of the *C. sativa* L. Extracts

The results of TPC and TFC of *C. sativa* L. extracts are presented in Tables S1 and S2 and Figure 1. Among the extracts, the inflorescence extract (CIF) exhibited the highest TPC (331.68 ± 2.96 mg GAE/g dry extract) and TFC (128.83 ± 2.33 mg QE/g dry extract). This was followed by the leaf extract (CLE) with a TPC of 227.82 ± 1.32 mg gallic acid/g extract and a TFC of 99.56 ± 1.34 mg QE/g extract. The root (CRO), stem (CST), and seed (CSE) extracts showed progressively lower TPC and TFC values, with the seed extract having the lowest phenolic content (22.62 ± 0.06 mg GAE/g dry extract) but a relatively high flavonoid content (111.49 ± 0.83 mg QE/g dry extract).

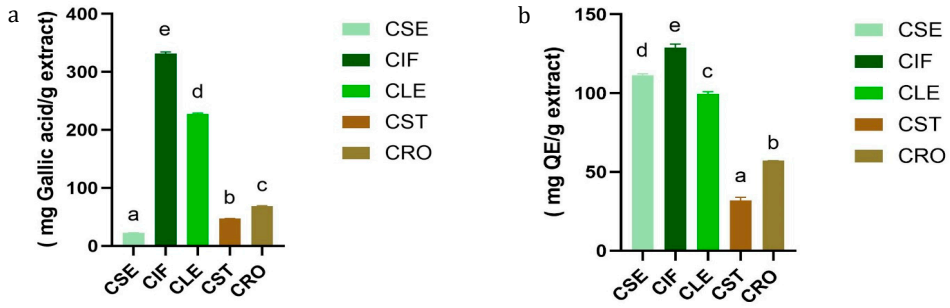

Figure 1. (**a**) TPC and (**b**) TFC comparison between five different parts of *C. sativa* L. Different letters indicated significant differences (p-value < 0.05).

These findings align with previous studies, such as those reported by Izzo et al. (2020) and Agarwal C. et al. (2018) [24,25] which also observed that the inflorescence of *C. sativa* L. contains a higher concentration of phenolic and flavonoid compounds compared to other plant parts. TPC values obtained in this study are considerably higher compared to those reported by Izzo et al., who documented TPC ranges between 10.51 and 52.58 mg GAE/g extract in inflorescence samples. This discrepancy can be attributed to differences in extraction solvents, with ethyl acetate possibly being more efficient in extracting a broader range of phenolic compounds compared to the methanol used in Izzo's study.

The variation in TPC and TFC values among the different plant parts may reflect the specific roles of these compounds in the plant's physiology. Inflorescences, as reproductive organs, likely accumulate higher levels of phenolics and flavonoids for protection against oxidative stress, whereas other parts, such as stems and roots, contain lower levels due to their different functional roles [26,27]. Interestingly, despite the lower phenolic content in the seed extract, its relatively high flavonoid content suggests that seeds might still offer valuable bioactive compounds for therapeutic applications, as supported by findings from Isidore, E. [28] on the antioxidant potential of different *C. sativa* L. extracts.

3.2.2. DPPH and NO Radical Scavenging Activities of the *C. sativa* L. Extracts

The antioxidant activities of *C. sativa* L. extracts were assessed using DPPH and NO radical scavenging assays, and the results are summarized in Table 2. The inflorescence (CIF) and leaf (CLE) ethyl acetate extracts demonstrated the highest activity against DPPH radicals among all extracts tested, with IC_{50} values of 3849.01 ± 5.25 µg/mL and 4709.98 ± 1.48 µg/mL, respectively. However, these IC_{50} values are substantially higher than those observed for ascorbic acid (IC_{50} = 40.41 ± 0.79 µg/mL), indicating that the antioxidant activity of these extracts is relatively weak. The other extracts (stem (CST), root (CRO), and seed (CSE)) did not achieve IC_{50} values, with inhibition percentages at 5 mg/mL ranging from 34.41 ± 1.58% for CST to 5.12 ± 0.93% for CSE (Table S3 and Figure S3). Similarly, in the NO radical scavenging assay, none of the *C. sativa* L. extracts reached IC_{50} values. The

CIF extract exhibited the highest inhibition at 1.25 mg/mL, with a value of 31.19 ± 0.96%, followed by CRO (29.42 ± 2.24%) and CLE (21.64 ± 2.51%) (Table S4 and Figure S4). These results suggest that while the CIF and CLE extracts have some capacity to scavenge radicals, their effectiveness is significantly lower compared to quercetin, which was used as a positive control (IC_{50} = 0.06 ± 0.00 µg/mL).

Table 2. Antioxidant activities of ethyl acetate extracts from five different parts of *C. sativa* L.

	Antioxidant Activities	
Extract	**DPPH, IC_{50} (µg/mL)**	**NO, IC_{50} (µg/mL)**
C. sativa L. seed (CSE)	-	-
C. sativa L. inflorescence (CIF)	3849.01 ± 5.25 [b]	-
C. sativa L. leaf (CLE)	4709.98 ± 1.48 [c]	-
C. sativa L. stem (CST)	-	-
C. sativa L. root (CRO)	-	-
Ascorbic acid	40.41 ± 0.79 [a]	NA
Quercetin	NA	0.06 ± 0.00

One-way ANOVA with Duncan test was used to compare the mean between samples, and different letters indicated significant differences (p-value < 0.05). NA = not applicable.

The variation in antioxidant activity across different parts of *C. sativa* L. can be attributed to the distinct bioactive compounds present in each part. In this study, the inflorescence and leaf extracts exhibited higher antioxidant activities, which is likely due to their higher concentrations of flavonoids and phenolic compounds. These compounds are well-known for their ability to neutralize free radicals and protect against oxidative stress, contributing significantly to the observed antioxidant properties [29]. The presence of these bioactive molecules is consistent with previous research [30], which demonstrated that the stem extract of *C. sativa* L., with the highest TPC and TFC, exhibited the strongest radical scavenging activity when compared to root and seed extracts. Additionally, Martyna Zagórska-Dziok et al. [15] showed that polyphenols and flavonoids are key contributors to the antioxidant properties of *C. sativa* L. extracts. However, although various phytochemicals present in *C. sativa* L., such as cannabidiol (CBD) and certain flavonoids, have been reported to exert nitric oxide (NO) scavenging or inhibitory effects in specific experimental settings, our crude extract did not demonstrate significant NO scavenging activity under the conditions used in this study. This apparent discrepancy may be attributed to low levels of these compounds or possible interactions within the extract that affect activity.

Despite the promising antioxidant activity observed in the inflorescence and leaf extracts, the overall performance of the extracts in both the DPPH and NO assays was relatively modest compared to standard antioxidants like ascorbic acid and quercetin. This suggests that while *C. sativa* L. extracts have some potential as natural antioxidants, they may require enhancement, such as through combination with more potent antioxidants, to achieve more effective results in therapeutic or cosmetic applications. Future studies involving the isolation and individual testing of key bioactive constituents, such as CBD, cannabigerol (CBG), and selected flavonoids, are warranted to better understand their specific roles in NO modulation.

3.3. 5-Lipoxygenase Inhibitory Activity of the C. sativa L. Extracts

The anti-inflammatory activity of the ethyl acetate extracts of *C. sativa* L. was evaluated using the human recombinant 5-lipoxygenase (5-LOX) inhibitory assay (Figure 2 and Table S5). The stem extract (CST) exhibited the highest inhibitory activity against 5-LOX, with an IC_{50} value of less than 0.024 µg/mL, surpassing the activity of the standard control, NDGA, which had an IC_{50} value of 0.48 ± 0.01 µg/mL (Figures S5 and S6). This was followed by

the inflorescence extract (CIF) with an IC_{50} of 2.39 ± 0.23 µg/mL, the leaf extract (CLE) with an IC_{50} of 4.62 ± 0.03 µg/mL, the root extract (CRO) with an IC_{50} of 8.04 ± 1.38 µg/mL, and the seed extract (CSE) with an IC_{50} of 9.44 ± 0.12 µg/mL. These results indicate that all *C. sativa* L. extracts exhibited inhibitory activity against 5-LOX, although the potency varied significantly among the different plant parts.

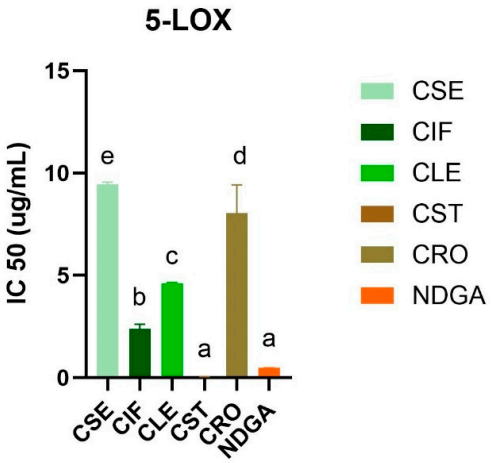

Figure 2. 5-LOX inhibitory activity (IC_{50}) of all *C. sativa* L. ethyl acetate extracts compared with a standard drug, NDGA. Different letters indicated significant differences (p-value < 0.05).

The enhanced activity of the stem extract could be linked to the presence of significant bioactive compounds, such as sitosterol and friedelin, which are known for their anti-inflammatory properties [31–33]. This finding is particularly noteworthy when compared with a previous study [34], which demonstrated that hemp seed hexane extracts (HSHE) effectively inhibit 5-LOX activity in sebocytes, reducing inflammation and lipid synthesis induced by *Propionibacterium acnes*. A previous study reported by Jin and colleagues highlighted that HSHE could inhibit 73% of 5-LOX levels in IGF-1-stimulated sebocytes, suggesting that hemp seeds are a potent source of anti-inflammatory agents. In addition, a previous study demonstrated the anti-inflammatory effects of cannabinoids, particularly cannabigerol (CBG) and cannabidiol (CBD), which have been shown to reduce reactive oxygen species levels and inhibit pro-inflammatory cytokine release more effectively than traditional antioxidants like vitamin C [35].

According to our results, the stem extract contained several compounds that possess 5-LOX inhibitory activity, notably friedelin. The previous study showed that friedelin isolated from *Commiphora berryi* exhibited potent inhibition against soybean lipoxygenase (IC_{50} = 35.8 µM) [36]. In our current study, the CST extract's performance against 5-LOX underscores the potential of the stem as an even more potent source of these bioactive compounds.

3.3.1. Tyrosinase Inhibitory Activity of the *C. sativa* L. Extracts

The anti-tyrosinase activity of *C. sativa* L. ethyl acetate extracts was assessed using a modified dopachrome method, with the results summarized in Table 3. The stem extract (CST) demonstrated the most potent tyrosinase inhibition, achieving an IC_{50} value of 0.01 ± 0.00 mg/mL. This was followed by the leaf extract (CLE), which had an IC_{50} value of 5.28 ± 1.98 mg/mL, and the root extract (CRO), with an IC_{50} value of 59.51 ± 8.95 mg/mL. In comparison, kojic acid, used as a positive control, demonstrated significantly stronger tyrosinase inhibition with an IC_{50} value of 0.004 ± 0.00 mg/mL. These findings align with previous research on the tyrosinase inhibitory activity of *C. sativa* L. extracts. A previous study by Manosroi et al. [37] reported that ethanolic extracts of *C. sativa* L. leaves and seeds exhibited significant tyrosinase inhibition with an IC_{50} value of 0.049 ± 0.02 mg/mL and

0.07 ± 0.06 mg/mL, respectively. This study pointed out that the antioxidant activity of *C. sativa* L. extracts may be attributed to the presence of tetrahydrocannabinol (THC), while their tyrosinase inhibitory effects could be linked to terpenoids and flavonoids. Similarly, Jae Kwon Kim et al. [38] reported that *N*-caffeoyltyramine, isolated from hemp seed extracts, exhibited melanogenesis inhibitory activity, indicating its potential for cosmetic applications as a skin-whitening agent. These studies suggested that both *C. sativa* L. leaves and seeds exhibit the promising anti-tyrosinase activity. However, our findings of seeds and leaves, which utilized ethyl acetate as the extraction solvent, showed lower anti-tyrosinase activity compared to the previous study. This discrepancy may be attributed to the more polar compounds extracted by ethanol in the earlier study, which likely contribute to its higher tyrosinase inhibition. In contrast, our ethyl acetate stem extract demonstrated superior anti-tyrosinase activity, possibly due to the composition of moderate polar compounds. This finding indicated that the stem was shown to be an underutilized source of bioactive compounds with significant potential. Eventually, the observed variations in activity can be attributed to several factors, including solvent and specific plant parts, underlining the importance of these factors for determining the biologically active components of the plant extracts.

Table 3. The anti-tyrosinase activity of the ethyl acetate extracts from five different parts of *C. sativa* L.

Extract	IC_{50} (mg/mL)
C. sativa L. seed (CSE)	>1000 ^{c}
C. sativa L. inflorescence (CIF)	>1000 ^{c}
C. sativa L. leaf (CLE)	5.28 ± 1.98 ^{a}
C. sativa L. stem (CST)	0.01 ± 0.00 ^{a}
C. sativa L. root (CRO)	59.51 ± 8.95 ^{b}
Kojic acid	0.004 ± 0.00 ^{a}

One-way ANOVA with Ducan's test was used to compare the mean between samples, and different letters indicated significant difference (p-value < 0.05).

3.3.2. Cytotoxicity on HaCaT Cells of the *C. sativa* L. Extracts

The cytotoxicity of *C. sativa* L. ethyl acetate extracts from various plant parts (seeds, inflorescences, leaves, stems, and roots) on HaCaT cell lines was evaluated using the MTT assay at concentrations of 5, 10, and 20 µg/mL, with etoposide serving as a standard cytotoxic drug for comparison. The results are depicted in Tables S6–S8 and Figure 3. At lower concentrations (5–10 µg/mL), all *C. sativa* L. extracts demonstrated non-toxic effects, with cell viability consistently exceeding 80%. This indicates that the extracts are safe for use at these concentrations. Notably, the *C. sativa* L. stem (CST) and seed (CSE) extracts maintained high cell viability even at the higher concentration of 20 µg/mL, with both showing more than 80% viability (CST: 92.79% ± 6.98%, CSE: 89.66% ± 5.21%). This suggests that these extracts are effective in supporting cell survival across a range of concentrations. In contrast, the other extracts (CIF, CLE, CRO) showed a decline in cell viability below 80% at 20 µg/mL, indicating that higher concentrations may reduce their safety profile.

Etoposide demonstrated non-cytotoxic effects at the lowest concentration (5 µg/mL) with a cell viability over 80%. However, as the concentration increased to 20 µg/mL, etoposide became significantly cytotoxic, reducing cell viability to 60.24 ± 9.13%. This finding contrasts prominently with the *C. sativa* L. extracts, particularly CST and CSE, which maintained higher cell viability even at the highest tested concentration, highlighting the relative safety of these plant extracts compared to a standard cytotoxic drug. The ability of these extracts to remain non-toxic and promote cell survival across a range of concentrations is particularly promising. However, the decline in viability observed with CIF, CLE, and

CRO at higher concentrations suggests that careful dosing and formulation are necessary to maximize the benefits of these extracts while minimizing potential cytotoxic effects.

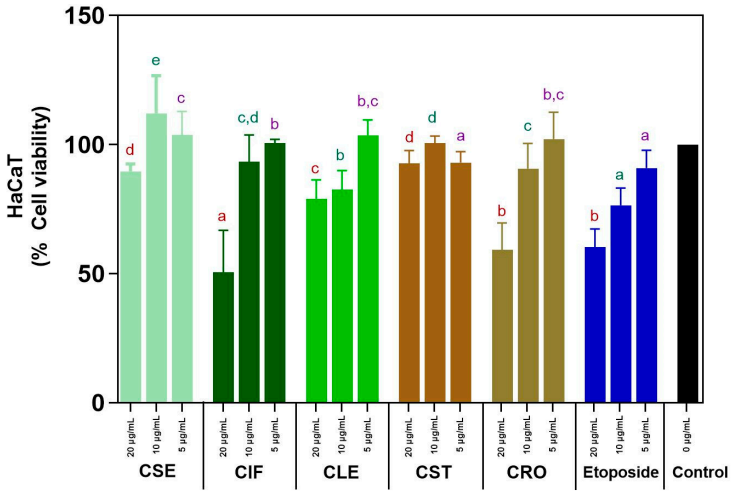

Figure 3. Cytotoxicity assay of all *C. sativa* L. ethyl acetate extracts and etoposide. Different letters indicated significant difference in the same concentration (p-value < 0.05). The same colors of the letters represent the same concentration across different parts for a comparison.

3.4. Chemical Analysis of Bioactive Compounds in the C. sativa L. Extracts by LC-QTOF-MS/MS and GC-MS/MS Techniques

The identification of compounds in five different parts of *C. sativa* L. ethyl acetate extracts was carried out using LC-QTOF-MS/MS and GC-MS/MS. The LC-QTOF-MS/MS system, operating under positive ionization mode, generated comprehensive total ion chromatograms (TICs) for each plant part, as shown in Figures S7–S11. Metabolites were tentatively identified based on a NIST database library score exceeding 95, and the key indicators supporting their identification are presented in Table 4. The analysis revealed the presence of 4 cannabinoids, 8 phenolic compounds, 2 flavonoids, 2 alkaloids, 5 saponins, and 14 terpenoids across the different plant parts. Notably, cannabinoids and alkaloids were exclusively found in the inflorescence (CIF) and leaf (CLE) extracts, while terpenoids and saponins were prevalent across all parts of the plant. Flavonoids were detected in all extracts except for the stem, and phenolic compounds were present in all except for the root (CRO) extract. GC-MS/MS further identified most of the compounds as neutral cannabinoids and lipids, as illustrated in Figure 4 and Tables S9–S13.

In the seed (CSE) ethyl acetate extract, GC-MS/MS identified fatty acids as the dominant compounds, with linoleic acid being particularly abundant. This finding aligns with previous studies that have established the seed's richness in polyunsaturated fatty acids (PUFAs), which include linoleic acid and its derivatives [22,39–41]. In contrast, LC-QTOF-MS/MS detected phenolic, flavonoid, saponin, and terpenoid compounds but did not identify any cannabinoids in the seed extract. This study demonstrated that different analytical techniques detect different bioactive compounds, such as fatty acids found in cannabis seeds. For example, linoleic acid was detected only by GC-MS/MS, but not by LC-MS. This is because GC-MS/MS is better suited for analyzing volatile and small molecules like fatty acids, especially when they are derivatized into esters. In contrast, LC-MS is more versatile for a broad spectrum of compounds and performs better with larger, more polar, or non-volatile molecules, making it less ideal for direct analysis of fatty acids unless they are chemically modified. These results suggest that while the seeds are a rich source of fatty acids, their contribution to cannabinoid content is minimal, highlighting the importance of selecting specific plant parts for desired bioactive compounds.

The inflorescence (CIF) extract, analyzed via GC-MS/MS, revealed dronabinol (THC) as the predominant bioactive compound, accounting for 49.7% of the total area, followed by cannabinol (CBN) at 11.96% and cannabichromene at 7.9%. Terpenes such as caryophyllene and phytol were also present in smaller amounts. LC-QTOF-MS/MS analysis further confirmed the diversity of bioactive compounds, including cannabinoids, phenolics, flavonoids, saponins, alkaloids, and terpenoids. The high cannabinoid content, particularly THC, is consistent with previous studies that have identified the inflorescence as a major source of cannabinoids, synthesized primarily in the glandular trichomes of female flowers [4,24]. This comprehensive profile underscores the inflorescence's potential for therapeutic applications, particularly in cannabinoid-based treatments. Although LC-QTOF-MS/MS analysis detected cannabidiolic acid (CBDA), it was not observed in the GC-MS/MS results. This discrepancy between the LC-MS and GC-MS analyses, such as the absence of CBDA in GC-MS, may be attributed to factors like incomplete decarboxylation, differences in detection limits, or the lack of derivatization and polarity mode optimization. These limitations will be addressed in future methodological improvements.

Table 4. Analysis of bioactive compound composition by LC-QTOF-MS/MS.

Major Classes	Bioactive Compound	Molecular Formula	Detected Ion	Exact Mass	*m/z*	Fragments	Retention Time (min)	Part of the Plant
Cannabinoids	Cannabigerol	$C_{21}H_{32}O_2$	$[M+H]^+$	316.2405	317.2472	123.0434, 193.1207	10.2772	Inflorescence (CIF), Leaf (CLE)
	Cannabidiolic acid	$C_{22}H_{30}O_4$	$[M+H]^+$	358.2136	359.2201	219.081, 261.1467	11.4921	Inflorescence (CIF), Leaf (CLE)
	Deta-11-tetrahydrocannabinol	$C_{21}H_{32}O_2$	$[M+H]^+$	315.2298	315.2291	193.1188, 259.1662	10.9532	Inflorescence (CIF), Leaf (CLE)
	Cannabinol	$C_{21}H_{26}O_2$	$[M+H]^+$	310.1936	311.2004	240.1141	8.9473	Leaf (CLE)
Phenolic compounds	Plantamajoside	$C_{29}H_{36}O_{15}$	$[M+H]^+$	662.3959	663.4027	529.2924	14.9209	Inflorescence (CIF)
	5,7-Dihydroxy-4-methylcoumarin	$C_{10}H_8O_4$	$[M+H]^+$	192.1156	193.1224	123.0437	11.7230	Inflorescence (CIF)
	3-Methoxybenzenepropanoic acid	$C_{10}H_{12}O_3$	$[M+H]^+$	180.1158	181.1225	179.1423	6.5724	Inflorescence (CIF)
	Pinoresinol	$C_{20}H_{22}O_6$	$[M+H]^+$	340.2594	341.2662	147.1165, 193.1310	10.3300	Leaf (CLE)
	6-hydroxy-4-methylcoumarin	$C_{10}H_8O_3$	$[M+H]^+$	176.1571	177.1639	-	5.4458	Leaf (CLE)
	2,6-Di-tert-butyl-4-hydroxymethylphenol	$C_{15}H_{24}O_2$	$[M+H]^+$	218.1677	219.1744	84.9591, 136.9312	5.9681	Stem (CST)
	Curculigoside	$C_{23}H_{32}O_{11}$	$[M+H]^+$	450.3564	489.3194	-	10.3229	Seed (CSE)
	Valeroyl salicylate	$C_{12}H_{14}O_3$	$[M+H]^+$	204.0792	205.0856	65.0385, 121.091, 149.0238	9.7979	Seed (CSE), Stem (CST)
Flavonoids	*N*-Isorhamnetin	$C_{16}H_{12}O_7$	$[M+H]^+$	316.1725	317.1792	-	10.7044	Inflorescence (CIF), Leaf (CLE), Seed (CSE)
	2′,5′-Dimethoxy-6-fluoroflavone	$C_{17}H_{13}FO_4$	$[M+H]^+$	300.1012	301.1394	-	9.7999	Leaf (CLE), Root (CRO)
Alkaloids	Vincamine	$C_{21}H_{26}N_2O_3$	[M+H]+	354.1834	355.1900	235.1116, 253.1232	11.2074	Inflorescence (CIF), Leaf (CLE)
	Thebaine	$C_{19}H_{21}NO_3$	$[M+H]^+$	311.1899	312.1966	146.0971, 282.1491	11.4521	Inflorescence (CIF), Leaf (CLE)
Saponins	Astrasieversianin XV	$C_{41}H_{68}O_{14}$	$[M+H]^+$	884.5466	923.5093	645.2117	31.2773	Inflorescence (CIF), Root (CRO), Stem (CST)
	Astragaloside II	$C_{41}H_{68}O_{14}$	$[M+H]^+$	848.6213	849.6283	-	13.5875	Root (CRO), Stem (CST)
	Astragaloside III	$C_{57}H_{92}O_{26}$	$[M+H]^+$	806.5739	807.5812	-	11.2879	Inflorescence (CIF), Leaf (CLE), Root (CRO), Seed (CSE), Stem (CST)
	Saikosaponin D	$C_{42}H_{68}O_{13}$	[M+H]+	762.6693	763.6756	149.1326, 189.1648	24.7425	Inflorescence (CIF), Leaf (CLE), Root (CRO), Seed (CSE), Stem (CST)
	Soyasaponin II	$C_{48}H_{78}O_{18}$	$[M+H]^+$	934.7231	935.7305	680.4992, 805.5938	38.0745	Seed (CSE)

Table 4. *Cont.*

Major Classes	Bioactive Compound	Molecular Formula	Detected Ion	Exact Mass	*m/z*	Fragments	Retention Time (min)	Part of the Plant
Terpenoids	Lupeol	$C_{30}H_{50}O$	$[M+H]^+$	408.3398	409.3833	95.0854, 135.1168, 161.1324	18.9885	Inflorescence (CIF), Leaf (CLE)
	alpha.-Cyperone	$C_{15}H_{22}O$	$[M+H]^+$	218.1680	219.1748	91.0541	8.1689	Inflorescence (CIF)
	Ç Curcumol	$C_{15}H_{26}O_2$	[M+H]+	236.1779	237.1847	151.1117, 179.1425	8.1093	Inflorescence (CIF), Leaf (CLE), Stem (CST)
	Lupenone	$C_{30}H_{48}O$	$[M+H]^+$	424.3715	425.3785	135.1167	13.3515	Inflorescence (CIF), Leaf (CLE), Root (CRO), Stem (CST)
	Farnesal	$C_{15}H_{24}O$	$[M+H]^+$	220.1836	221.1902	81.0697, 105.0698	9.7006	Inflorescence (CIF), Leaf (CLE)
	Steviolbioside	$C_{38}H_{60}O_{18}$	$[M+H]^+$	664.4172	665.4251	149.0250, 271.1844	10.2717	Inflorescence (CIF)
	Friedelin	$C_{30}H_{50}O$	$[M+H]^+$	426.3480	427.3572	173.0966, 325.3103	17.0872	Inflorescence (CIF), Leaf (CLE), Root (CRO), Stem (CST)
	Kahweol palmitate	$C_{40}H_{58}O_4$	$[M+H]^+$	534.2623	535.2700	-	12.2929	Leaf (CLE), Root (CRO)
	Aristolone	$C_{15}H_{22}O$	$[M+H]^+$	218.1680	219.1748	84.9600, 136.9313, 161.1330	8.1759	Root (CRO), Seed (CSE)
	Cucurbitacin E-2-*O*-glucoside	$C_{38}H_{58}O_{11}$	$[M+H]^+$	740.3889	741.3955	313.0734, 413.1930	11.5132	Leaf (CLE)
	Kahweol	$C_{20}H_{26}O_3$	$[M+H]^+$	314.2242	315.2320	-	12.0785	Root (CRO)
	Uvaol	$C_{30}H_{50}O_2$	$[M+H]^+$	410.3555	443.3885	95.0857, 177.9638	13.5105	Root (CRO)
	Cycloartenol acetate	$C_{32}H_{52}O_2$	$[M+H]^+$	408.3768	409.3832	137.1325, 271.2415	20.7737	Root (CRO)
	Betulin	$C_{30}H_{50}O_2$	$[M+H]^+$	442.3820	443.3886	177.1636, 229.1945	13.5390	Stem (CST)

The leaf (CLE) extract also showed significant cannabinoid content, with dronabinol and cannabinol being the most prominent compounds identified by GC-MS/MS. Other notable constituents included nonacosane, γ-sitosterol, and various terpenoids. LC-QTOF-MS/MS analysis confirmed the presence of a broad range of bioactive compounds, including phenolics, flavonoids, saponins, alkaloids, and terpenoids. These findings align with previous research that has characterized cannabis leaves as rich in alkaloids, flavonoids, and phenolics, though the presence of saponins was not previously reported [42,43]. The diverse bioactive profile of the leaf extract suggests its potential for multiple therapeutic applications, including anti-inflammatory and antioxidant therapies.

In contrast, the stem (CST) extract was dominated by sterols and triterpenoids, with γ-sitosterol being the most abundant compound identified by GC-MS/MS. Other significant compounds included campesterol, friedelinol, and stigmasterol. LC-QTOF-MS/MS analysis did not detect cannabinoids in the stem extract, which is consistent with previous studies indicating that cannabinoids are either absent or present only in trace amounts in the stem [30,34]. Several compounds found in stem extract are known as anti-inflammatory agents, including betulin [44], friedelin [31], lupenone [45], and curcumol [46]. In addition, betulin has been reported to exhibit the highest anti-inflammatory activity in models of murine ear edema and skin inflammation [44]. Notably, betulin was exclusively identified in the stem extract of cannabis, which may partly explain the superior anti-inflammatory activity observed in this plant part compared to others. These findings suggest that cannabis stem extract holds potential as a skincare ingredient due to its capacity to mitigate cellular inflammation. Lupenone, identified in multiple parts of the cannabis plant in our study, has also been recognized as a bioactive compound with anti-inflammatory properties. Previous research has demonstrated that lupenone may help prevent a range of inflammatory and oxidative stress-related disorders [45]. The presence of these bioactive sterols and triter-

penoids suggests that the stem, often considered a waste product, may have underexplored therapeutic potential, particularly in anti-inflammatory and antioxidant applications.

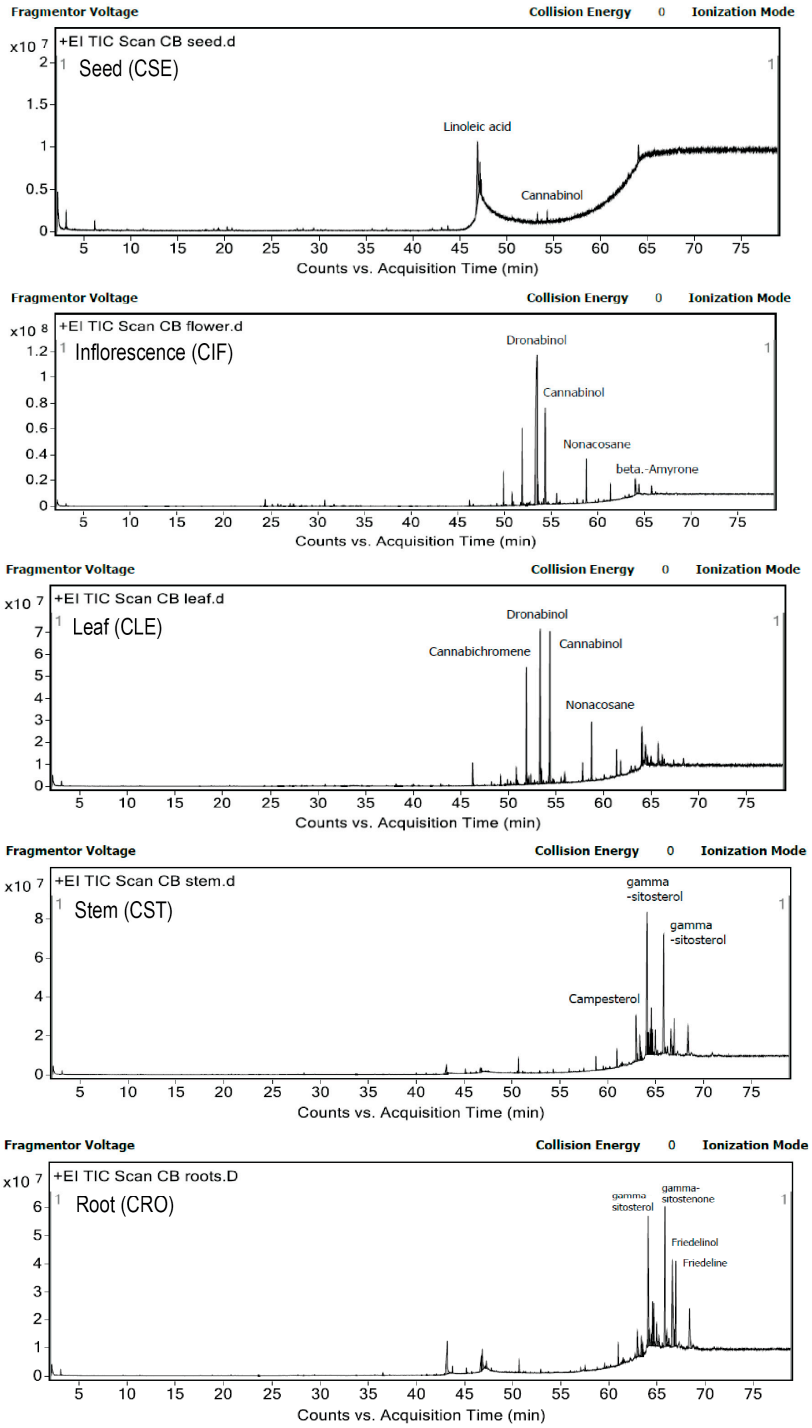

Figure 4. Chromatograms of five different parts of *C. sativa* L. ethyl acetate extracts were detected by gas chromatography—mass spectrometry method.

The root (CRO) extract was notably devoid of cannabinoids, with the primary compounds identified by GC-MS/MS being γ-sitostenone, γ-sitosterol, and friedelin. LC-QTOF-MS/MS analysis confirmed the presence of flavonoids, saponins, and terpenoids, but again, no cannabinoids were detected. This finding is consistent with previous studies that have identified the root as a rich source of sterols and triterpenoids, rather than cannabinoids [47,48]. The root's unique bioactive profile, including compounds like friedelin and

4-campestene-3-one, supports its potential use in formulations targeting inflammation and oxidative stress.

A particularly significant finding of this study is the observation that the stem, despite its lower antioxidant activity compared to the inflorescence, exhibited substantial anti-inflammatory and anti-tyrosinase activities. This challenges the common assumption that antioxidant activity is directly correlated with anti-inflammatory and anti-melanogenic effects. The data suggest that bioactive compounds other than flavonoids and phenolics may play a critical role in these activities, highlighting the complexity of plant bioactivity and the need for a more nuanced understanding of how different compounds contribute to therapeutic effects. Moreover, while seed oil is often promoted for its anti-aging, anti-acne, and anti-freckle properties, our findings suggest that the seed extract may have limited efficacy in these areas compared to other parts of the plant. Although this study focused on qualitative chemical profiling, future investigations should consider quantitative analysis, including calibration with pure standards and multivariate approaches such as PCA, to correlate compound concentrations, particularly sterols and triterpenoids, with observed biological activities.

4. Conclusions

In conclusion, this study elucidates the distinct bioactive profiles and pharmacological potentials of various parts of *C. sativa* L., highlighting their potential applications in pharmaceutical and cosmetic industries. The results reveal that the seed extract of *C. sativa* L. (CSE) provides the highest yield, primarily due to its fatty acid-rich composition. The inflorescence extract (CIF), on the other hand, exhibits significant antioxidant properties, along with high total phenolic and flavonoid content, indicating its potential for therapeutic use against oxidative stress-related conditions. Notably, the stem extract (CST) demonstrates the most potent enzyme inhibitory activity, particularly against 5-lipoxygenase and tyrosinase, comparable to standard drugs in efficacy. The absence of cytotoxicity in HaCaT cells further supports the safety of these extracts at specific concentrations, suggesting their viability for skin-related applications. The identification of key bioactive compounds, such as phenolic and terpenoid in the stem (CST) extracts, underscores the anti-inflammatory, anti-tyrosinase, and antioxidant activities associated with these parts of the plant. Notably, the discovery of friedelin and especially betulin in the stem (CST) extracts warrants further investigation due to its potential antitumor, anticancer, and anti-inflammatory properties. The study suggests that the *C. sativa* L. stem (CST), often considered a waste product, could be a valuable resource for the development of nutraceuticals or cosmeceuticals aimed at addressing skin aging and related conditions. However, additional in cell, in vivo, and clinical studies in accordance with skin aging management are necessary to substantiate these preliminary findings and explore the therapeutic potential of *C. sativa* L. in greater depth. Furthermore, chemometric profiling techniques such as principal component analysis are recommended for future studies to explore which groups of compounds are primarily associated with the bioactivity.

Supplementary Materials: The following supporting information can be downloaded at: https://www.mdpi.com/article/10.3390/sci7020077/s1, Table S1 The total phenolic content of the *Cannabis sativa* L. extracts; Table S2 The total flavonoid content of the *Cannabis sativa* L. extracts; Table S3 The radical scavenging percentage inhibition against DPPH of ethyl acetate extracts from five different parts of *Cannabis sativa* L; Table S4 The nitric oxide (NO) radical scavenging activity of ethyl acetate extracts from five different parts of *Cannabis sativa* L.; Table S5 Anti-inflammatory activity against human recombinant 5-LOX of ethyl acetate extracts from five different parts of *Cannabis sativa* L.; Table S6 Percent cell viability of HaCaT cells treated with *Cannabis sativa* L. ethyl acetate extracts (5 µg/mL); Table S7 Percent cell viability of HaCaT cells treated with *Cannabis sativa* L. ethyl acetate

extracts (10 µg/mL); Table S8 Percent cell viability of HaCaT cells treated with *Cannabis sativa* L. ethyl acetate extracts (20 µg/mL); Table S9 Volatile compounds of the *Cannabis sativa* L. seed (CSE) ethyl acetate extract by GC-MS/MS; Table S10 Volatile compounds of the *Cannabis sativa* L. inflorescence (CIF) ethyl acetate extract by GC-MS/MS; Table S11 Volatile compounds of the *Cannabis sativa* L. leaf (CLF) ethyl acetate extract by GC-MS/MS; Table S12 Volatile compounds of the *Cannabis sativa* L. stem (CST) ethyl acetate extract by GC-MS/MS; Table S13 Volatile compounds of the *Cannabis sativa* L. root (CRO) ethyl acetate extract by GC-MS/MS; Figure S1 Gallic acid calibration curve for quantification of the total phenolic content; Figure S2 Quercetin concentration calibration curve for quantification of the total flavonoid content; Figure S3 The radical scavenging percentage inhibition of *Cannabis sativa* L. extracts against DPPH radicals; Figure S4 The percentage inhibition of *Cannabis sativa* L. extracts against nitric oxide radicals; Figure S5 5-LOX inhibitory activity (IC50) of *Cannabis sativa* L. ethyl acetate extracts; Figure S6 5-LOX inhibitory activity (IC50) of NDGA as a positive control; Figure S7 Chromatogram of *Cannabis sativa* L. seed ethyl acetate extract detected by LC-QTOF-MS/MS; Figure S8 Chromatogram of *Cannabis sativa* L. inflorescence ethyl acetate extract detected by LC-QTOF-MS/MS; Figure S9 Chromatogram of *Cannabis sativa* L. leaf ethyl acetate extract detected by LC-QTOF-MS/MS; Figure S10 Chromatogram of *Cannabis sativa* L. stem ethyl acetate extract detected by LC-QTOF-MS/MS; Figure S11 Chromatogram of *Cannabis sativa* L. root ethyl acetate extract detected by LC-QTOF-MS/MS.

Author Contributions: Conceptualization, P.K., A.P. and C.A.; methodology, P.K. and A.P.; validation, P.K., A.P. and C.A.; formal analysis, P.K., D.L. and H.M.; investigation, P.K., D.L. and H.M.; data curation, P.K., D.L. and H.M.; writing—original draft preparation, P.K. and A.P.; writing—review and editing, P.K., D.L., H.M., A.P. and C.A.; supervision, A.P. and C.A.; funding acquisition, P.K. All authors have read and agreed to the published version of the manuscript.

Funding: This research was funded by the 90th Anniversary of Chulalongkorn University Scholarship, Ratchadapisek Sompotch Fund.

Institutional Review Board Statement: Not applicable.

Informed Consent Statement: Not applicable.

Data Availability Statement: The data that support the findings of this study are available in the manuscript and Supplementary Information.

Use of Artificial Intelligence: During the development of this manuscript, the authors employed tools such as ChatGPT (GPT-4o) and QuillBot to improve clarity and language quality. Following their use, the authors carefully reviewed and edited the content to ensure accuracy and originality, and take full responsibility for the final version of the manuscript.

Acknowledgments: We extend our gratitude to the laboratory technicians at the College of Public Health Sciences, Chulalongkorn University, for their valuable instrumental assistance.

Conflicts of Interest: The authors declare no conflicts of interest.

References

1. Poljšak, B.; Dahmane, R. Free radicals and extrinsic skin aging. *Dermatol. Res. Pract.* **2012**, *2012*, 135206. [CrossRef] [PubMed]
2. Masaki, H. Role of antioxidants in the skin: Anti-aging effects. *J. Dermatol. Sci.* **2010**, *58*, 85–90. [CrossRef] [PubMed]
3. Andra, C.; Suwalska, A.; Dumitrescu, A.M.; Kerob, D.; Delva, C.; Hasse-Cieślińska, M.; Solymosi, A.; Arenbergerova, M. A Corrective Cosmetic Improves the Quality of Life and Skin Quality of Subjects with Facial Blemishes Caused by Skin Disorders. *Clin. Cosmet. Investig. Dermatol.* **2020**, *13*, 253–257. [CrossRef]
4. Skala, T.; Kahánková, Z.; Tauchen, J.; Janatová, A.; Klouˇcek, P.; Hubka, V.; Fraˇnková, A. Medical cannabis dimethyl ether, ethanol and butane extracts inhibit the in vitro growth of bacteria and dermatophytes causing common skin diseases. *Front. Microbiol.* **2022**, *13*, 953092. [CrossRef]
5. Di Costanzo, L.F. Structural characterization of tyrosinases and an update on human enzymes. *Enzymes* **2024**, *56*, 55–83. [CrossRef]
6. Mukherjee, P.K.; Biswas, R.; Sharma, A.; Banerjee, S.; Biswas, S.; Katiyar, C.K. Validation of medicinal herbs for anti-tyrosinase potential. *J. Herb. Med.* **2018**, *14*, 1–16. [CrossRef]

7. Ando, H.; Kondoh, H.; Ichihashi, M.; Hearing, V.J. Approaches to identify inhibitors of melanin biosynthesis via the quality control of tyrosinase. *J. Investig. Dermatol.* **2007**, *127*, 751–761. [CrossRef]
8. Muddathir, A.M.; Yamauchi, K.; Batubara, I.; Mohieldin, E.A.M.; Mitsunaga, T. Anti-tyrosinase, total phenolic content and antioxidant activity of selected Sudanese medicinal plants. *S. Afr. J. Bot.* **2017**, *109*, 9–15. [CrossRef]
9. Ma, W.; Wlaschek, M.; Tantcheva-Poór, I.; Schneider, L.A.; Naderi, L.; Razi-Wolf, Z.; Schüller, J.; Scharffetter-Kochanek, K. Chronological ageing and photoageing of the fibroblasts and the dermal connective tissue. *Clin. Exp. Dermatol.* **2001**, *26*, 592–599. [CrossRef]
10. Khojah, H.; Ahmed, S.R.; Alharbi, S.Y.; AlSabeelah, K.K.; Alrayyes, H.Y.; Almusayyab, K.B.; Alrawiliy, S.R.; Alshammari, R.M.; Qasim, S. Skin anti-aging potential of Launaea procumbens extract: Antioxidant and enzyme inhibition activities supported by ADMET and molecular docking studies. *Saudi Pharm. J.* **2024**, *32*, 102107. [CrossRef]
11. Podder, D.; Sasmal, S.; Haldar, D. Sonication Responsive Gelator: Synthesis and Applications. *Curr. Org. Synth.* **2015**, *12*, 440–456. [CrossRef]
12. French, J.A.; Koepp, M.; Naegelin, Y.; Vigevano, F.; Auvin, S.; Rho, J.M.; Rosenberg, E.; Devinsky, O.; Olofsson, P.S.; Dichter, M.A. Clinical studies and anti-inflammatory mechanisms of treatments. *Epilepsia* **2017**, *58* (Suppl. S3), 69–82. [CrossRef]
13. Huang, S.; Li, H.; Xu, J.; Zhou, H.; Seeram, N.P.; Ma, H.; Gu, Q. Chemical constituents of industrial hemp roots and their anti-inflammatory activities. *J. Cannabis Res.* **2023**, *5*, 1. [CrossRef] [PubMed]
14. Rea Martinez, J.; Montserrat-de la Paz, S.; De la Puerta, R.; García-Giménez, M.D.; Fernández-Arche, M.Á. Characterization of bioactive compounds in defatted hempseed (*Cannabis sativa* L.) by UHPLC-HRMS/MS and anti-inflammatory activity in primary human monocytes. *Food Funct.* **2020**, *11*, 4057–4066. [CrossRef]
15. Zagórska-Dziok, M.; Bujak, T.; Ziemlewska, A.; Nizioł-Łukaszewska, Z. Positive Effect of *Cannabis sativa* L. Herb Extracts on Skin Cells and Assessment of Cannabinoid-Based Hydrogels Properties. *Molecules* **2021**, *26*, 802. [CrossRef] [PubMed]
16. Rinnerthaler, M.; Bischof, J.; Streubel, M.K.; Trost, A.; Richter, K. Oxidative stress in aging human skin. *Biomolecules* **2015**, *5*, 545–589. [CrossRef]
17. Rožanc, J.; Kotnik, P.; Milojević, M.; Gradišnik, L.; Knez Hrnčič, M.; Knez, Ž.; Maver, U. Different *Cannabis sativa* Extraction Methods Result in Different Biological Activities against a Colon Cancer Cell Line and Healthy Colon Cells. *Plants* **2021**, *10*, 566. [CrossRef]
18. Liana, D.; Eurtivong, C.; Phanumartwiwath, A. Boesenbergia rotunda and Its Pinostrobin for Atopic Dermatitis: Dual 5-Lipoxygenase and Cyclooxygenase-2 Inhibitor and Its Mechanistic Study through Steady-State Kinetics and Molecular Modeling. *Antioxidants* **2024**, *13*, 74. [CrossRef]
19. Manosroi, A.; Boonpisuttinant, K.; Winitchai, S.; Manosroi, W.; Manosroi, J. Free radical scavenging and tyrosinase inhibition activity of oils and sericin extracted from Thai native silkworms (*Bombyx mori*). *Pharm. Biol.* **2010**, *48*, 855–860. [CrossRef]
20. Wan, L.; Song, Z.; Wang, Z.; Dong, J.; Chen, Y.; Hu, J. Repair effect of *Centella asiatica* (L.) extract on damaged HaCaT cells studied by atomic force microscopy. *J. Microsc.* **2023**, *292*, 148–157. [CrossRef]
21. Ibrahim, E.A.; Wang, M.; Radwan, M.M.; Wanas, A.S.; Majumdar, C.G.; Avula, B.; Wang, Y.H.; Khan, I.A.; Chandra, S.; Lata, H.; et al. Analysis of Terpenes in *Cannabis sativa* L. Using GC/MS: Method Development, Validation, and Application. *Planta Med.* **2019**, *85*, 431–438. [CrossRef] [PubMed]
22. Delgado-Povedano, M.M.; Sánchez-Carnerero Callado, C.; Priego-Capote, F.; Ferreiro-Vera, C. Untargeted characterization of extracts from *Cannabis sativa* L. cultivars by gas and liquid chromatography coupled to mass spectrometry in high resolution mode. *Talanta* **2020**, *208*, 120384. [CrossRef] [PubMed]
23. Michailidis, D.; Angelis, A.; Nikolaou, P.E.; Mitakou, S.; Skaltsounis, A.L. Exploitation of Vitis vinifera, Foeniculum vulgare, *Cannabis sativa* and *Punica granatum* By-Product Seeds as Dermo-Cosmetic Agents. *Molecules* **2021**, *26*, 731. [CrossRef] [PubMed]
24. Izzo, L.; Castaldo, L.; Narváez, A.; Graziani, G.; Gaspari, A.; Rodríguez-Carrasco, Y.; Ritieni, A. Analysis of Phenolic Compounds in Commercial *Cannabis sativa* L. Inflorescences Using UHPLC-Q-Orbitrap HRMS. *Molecules* **2020**, *25*, 631. [CrossRef]
25. Agarwal, C.; Máthé, K.; Hofmann, T.; Csóka, L. Ultrasound-Assisted Extraction of Cannabinoids from *Cannabis Sativa* L. Optimized by Response Surface Methodology. *J. Food Sci.* **2018**, *83*, 700–710. [CrossRef]
26. Ghosh, D.; Chaudhary, N.; Shanker, K.; Kumar, B.; Kumar, N. Monoecious Cannabis sativa L. discloses the organ-specific variation in glandular trichomes, cannabinoids content and antioxidant potential. *J. Appl. Res. Med. Aromat. Plants* **2023**, *35*, 100476. [CrossRef]
27. Maina, S.; Ryu, D.H.; Bakari, G.; Misinzo, G.; Nho, C.W.; Kim, H.Y. Variation in Phenolic Compounds and Antioxidant Activity of Various Organs of African Cabbage (*Cleome gynandra* L.) Accessions at Different Growth Stages. *Antioxidants* **2021**, *10*, 1952. [CrossRef]
28. Isidore, E.; Karim, H.; Ioannou, I. Extraction of Phenolic Compounds and Terpenes from *Cannabis sativa* L. By-Products: From Conventional to Intensified Processes. *Antioxidants* **2021**, *10*, 942. [CrossRef]
29. Yu, M.; Gouvinhas, I.; Rocha, J.; Barros, A.I. Phytochemical and antioxidant analysis of medicinal and food plants towards bioactive food and pharmaceutical resources. *Sci. Rep.* **2021**, *11*, 10041. [CrossRef]

30. Kim, Y.N.; Sim, K.S.; Park, S.; Sohn, H.Y.; Kim, T.; Kim, J.H. In Vitro and In Vivo Anti-Inflammatory Effects of *Cannabis sativa* Stem Extract. *J. Med. Food* **2022**, *25*, 408–417. [CrossRef]
31. Radi, M.H.; El-Shiekh, R.A.; El-Halawany, A.M.; Abdel-Sattar, E. Friedelin and 3β-Friedelinol: Pharmacological Activities. *Rev. Bras. Farmacog.* **2023**, *33*, 886–900. [CrossRef]
32. Rashed, K. Beta-sitosterol medicinal properties: A review article. *J. Sci. Innov. Technol.* **2020**, *9*, 208–212.
33. Da Marinho, A.M.N.; da Silva Neto, R.W.G. Anti-inflammatory effects of cannabinoids. *BrJP* **2023**, *6*, 31–37. [CrossRef]
34. Jin, S.; Lee, M.-Y. The ameliorative effect of hemp seed hexane extracts on the Propionibacterium acnes-induced inflammation and lipogenesis in sebocytes. *PLoS ONE* **2018**, *13*, e0202933. [CrossRef]
35. Perez, E.; Fernandez, J.R.; Fitzgerald, C.; Rouzard, K.; Tamura, M.; Savile, C. In Vitro and Clinical Evaluation of Cannabigerol (CBG) Produced via Yeast Biosynthesis: A Cannabinoid with a Broad Range of Anti-Inflammatory and Skin Health-Boosting Properties. *Molecules* **2022**, *27*, 491. [CrossRef]
36. Kumari, R.; Meyyappan, A.; Selvamani, P.; Mukherjee, J.; Jaisankar, P. Lipoxygenase inhibitory activity of crude bark extracts and isolated compounds from *Commiphora berryi*. *J. Ethnopharmacol.* **2011**, *138*, 256–259. [CrossRef]
37. Manosroi, A.; Chankhampan, C.; Kietthanakorn, B.O.; Ruksiriwanich, W.; Chaikul, P.; Boonpisuttinant, K.; Sainakham, M.; Manosroi, W.; Tangjai, T.; Manosroi, J. Pharmaceutical and cosmeceutical biological activities of hemp (*Cannabis sativa* L. var. sativa) leaf and seed extracts. *Chiang Mai J. Sci.* **2019**, *46*, 180–195.
38. Kim, J.K.; Heo, H.-Y.; Park, S.; Kim, H.; Oh, J.J.; Sohn, E.-H.; Jung, S.-H.; Lee, K. Characterization of Phenethyl Cinnamamide Compounds from Hemp Seed and Determination of Their Melanogenesis Inhibitory Activity. *ACS Omega* **2021**, *6*, 31945–31954. [CrossRef]
39. Citti, C.; Linciano, P.; Russo, F.; Luongo, L.; Iannotta, M.; Maione, S.; Laganà, A.; Capriotti, A.L.; Forni, F.; Vandelli, M.A.; et al. A novel phytocannabinoid isolated from *Cannabis sativa* L. with an in vivo cannabimimetic activity higher than Δ(9)-tetrahydrocannabinol: Δ(9)-Tetrahydrocannabiphorol. *Sci. Rep.* **2019**, *9*, 20335. [CrossRef]
40. Ross, S.A.; Mehmedic, Z.; Murphy, T.P.; Elsohly, M.A. GC-MS analysis of the total Δ9-THC content of both drug- and fiber-type cannabis seeds. *J. Anal. Toxicol.* **2000**, *24*, 715–717. [CrossRef]
41. Kitamura, M.; Kiba, Y.; Suzuki, R.; Tomida, N.; Uwaya, A.; Isami, F.; Deng, S. Cannabidiol Content and In Vitro Biological Activities of Commercial Cannabidiol Oils and Hemp Seed Oils. *Medicines* **2020**, *7*, 57. [CrossRef] [PubMed]
42. Kubiliene, A.; Mickute, K.; Baranauskaite, J.; Marksa, M.; Liekis, A.; Sadauskiene, I. The Effects of *Cannabis sativa* L. Extract on Oxidative Stress Markers In Vivo. *Life* **2021**, *11*, 647. [CrossRef]
43. Nakkliang, K.; Areesantichai, C.; Rungsihirunrat, K. Assessment of pharmacognostic specification of *Cannabis sativa* leaves in Thailand. *J. Adv. Pharm. Technol. Res.* **2022**, *13*, 226–231. [CrossRef]
44. Hordyjewska, A.; Ostapiuk, A.; Horecka, A.; Kurzepa, J. Betulin and betulinic acid: Triterpenoids derivatives with a powerful biological potential. *Phytochem. Rev.* **2019**, *18*, 929–951. [CrossRef]
45. Xu, F.; Huang, X.; Wu, H.; Wang, X. Beneficial health effects of lupenone triterpene: A review. *Biomed. Pharmacother.* **2018**, *103*, 198–203. [CrossRef]
46. Chen, X.; Zong, C.; Gao, Y.; Cai, R.; Fang, L.; Lu, J.; Liu, F.; Qi, Y. Curcumol exhibits anti-inflammatory properties by interfering with the JNK-mediated AP-1 pathway in lipopolysaccharide-activated RAW264.7 cells. *Eur. J. Pharmacol.* **2014**, *723*, 339–345. [CrossRef] [PubMed]
47. Kornpointner, C.; Sainz Martinez, A.; Marinovic, S.; Haselmair-Gosch, C.; Jamnik, P.; Schröder, K.; Löfke, C.; Halbwirth, H. Chemical composition and antioxidant potential of *Cannabis sativa* L. roots. *Ind. Crop. Prod.* **2021**, *165*, 113422. [CrossRef]
48. Javaid, A.; Khan, I.H.; Ferdosi, M.F. Bioactive constituents of wild *Cannabis sativa* roots from Pakistan. *Pak. J. Weed Sci. Res.* **2021**, *27*, 359. [CrossRef]